Journal of the European Ceramic Society 15 (1995) 867–874

0955-2219(95)00050-X
0955-2219/95/$9.50

Electrical and Thermal Transport Properties of (La,Ca)(Cr,Co)O_3

Rasit Koc[a] & Harlan U. Anderson[b]

[a]Southern Illinois University, Department of Mechanical Engineering and Energy Processes, Carbondale, IL 62901, USA
[b]University of Missouri-Rolla, Ceramic Engineering Department, Rolla, MO 65401, USA

(Received 19 September 1994; revised version received 14 February 1995; accepted 20 February 1995)

Abstract

DC electrical conductivity and Seebeck data as functions of temperature and oxygen activity were used to explain the electrical and thermal transport properties of (La,Ca)(Cr,Co)O_3. The electrical conductivity data of La(Cr,Co)O_3 suggested that it depends upon Co content. At Co concentrations less than 20 mol%, Co acted as traps for the carriers and decreased the electrical conductivity of the compositions at temperatures less than 900°C. As the Co concentration increased to above 20 mol%, electrical conductivity increased significantly due to a connecting path of available Co sites. Additional Ca substitution for La increased the electrical conductivity in accordance with Verway's principle. Defect models derived from the electrical conductivity data were found to relate the carrier concentrations to the Ca, Co and oxygen vacancy concentrations. The measured Seebeck coefficients were found to be positive even for the most reducing conditions, indicating that (La,Ca)(Cr,Co)O_3 compositions with Co ≤ 0·3 and Ca ≤ 0·3 were as stable as $LaCrO_3$. The Heikes formula was adopted to interpret the Seebeck coefficient results. These results indicated that electrical conduction in La(Cr,Co)O_3 and (La,Ca)(Cr,Co)O_3 occurs via the non-adiabatic and adiabatic small polaron mechanisms, respectively.

1 Introduction

The demand for materials that possess the chemical stability and electrical conductivity required in high-temperature solid oxide fuel cells (SOFC) and oxygen-separation cells has led to the investigation of the substantially mixed perovskite-type (La,Ca)(Cr,Co)O_3 system.[1,2] The basic perovskite crystal structure is given by the formula ABO_3 in which A, the large cation site, may be an alkali, alkaline earth, or rare earth ion and B represents a transition metal cation. The (La,Ca)(Cr,Co)O_3 system has a pseudo-perovskite crystal structure because its crystal structure deviates from the ideal cubic perovskite structure, (i.e. orthorhombic and rhombohedral). This system is composed of both Cr and Co B-site ions in an attempt to retain the desirable properties found in the end members, (e.g. $LaCrO_3$ — chemical stability in both air and in highly reducing atmospheres at 1000°C, $LaCoO_3$ — high electrical conductivity and sinterability). Ca is substituted for a fraction of the La on the A lattice site, in order to increase the small-polaron carrier concentration according to the Verway controlled ionic valency principle.

Both $LaCrO_3$ and $LaCoO_3$ are believed to show a thermally activated electrical conductivity due to p-type small-polaron hopping among B-site cations. $LaCrO_3$ is chemically stable to high temperatures over a wide range of oxygen activity. $LaCoO_3$ has a significantly greater electrical conductivity than $LaCrO_3$. However, $LaCoO_3$ is not chemically stable under reducing conditions at high temperatures.

The present author's recent results on $La_{1-x}Ca_xCr_{1-y}Co_yO_3$ have shown that compositions with $x \geq 0{\cdot}1$ and $y \geq 0{\cdot}1$ can be sintered to densities above 94% of theoretical in air at 1400°C and below.[1] The electrical conductivity as measured in air from room temperature to 1100°C increased with increasing Co and Ca content. At 1000°C, values from 1·5 S/cm (for $LaCr_{0.9}Co_{0.1}O_3$) to 50 S/cm (for $La_{0.7}Ca_{0.3}Cr_{0.9}Co_{0.1}O_3$) were measured.[2] However, the room-temperature electrical conductivity minima occurs at a Co concentration of approximately 20%. The Seebeck coefficients were positive, indicating p-type conductivity. The substitution of Co for Cr significantly decreased the Seebeck coefficients, indicating that Co substitution for Cr increased the carrier concentration. Additional Ca substitution for La resulted in a further decrease in the Seebeck coefficient.

Seebeck coefficients then exhibited a temperature-independent behavior, indicating that the carrier mobility, rather than carrier concentration, was thermally activated.[2] However, published works regarding the electrical behavior with respect to oxygen activity of $(La,Ca)(Cr,Co)O_3$ ceramics are virtually non-existent.

The objectives of the present paper are to explain the electrical and thermal transport properties of $(La,Ca)(Cr,Co)O_3$ ceramics and provide information on electrical conductivity and Seebeck coefficients as a function of oxygen activity for the material system at 1000°C.

2 Experimental Procedure

Specimens in the $(La,Ca)(Cr,Co)O_3$ system were prepared by a polymer precursor method similar to that first described by Pechini.[3] The starting chemicals were reagent-grade materials and were standardized by thermogravimetric methods to determine the actual cation contents. The desired compositions were prepared by dissolving measured amounts of selected carbonates and nitrates in solutions of citric acid, ethylene glycol, and water. The mixtures were heated on a hot plate at about 95°C until polymerization had occurred. Subsequent heating at higher temperatures resulted in the decomposition of the polymer resin and allowed conversion into the desired oxide. Final calcination was done at 850°C for 8 h. The resulting powders were milled and subjected to X-ray diffraction to ensure that they were single-phase. Samples for electrical conductivity and Seebeck measurements were formed by dry pressing at 2500 kg/cm^2 and then sintering the compacts at 1500°C for 10 h in a SiC heated furnace. Bulk densities of about 95% of theoretical were obtained. Rectangular specimens, usually 0·3 × 0·3 × 2 cm, were cut from the sintered bars. To reduce the effects of barrier layers and non-ohmic contacts, Pt paste was applied to the contact faces of the specimens.

Four-wire DC electrical-conductivity and Seebeck measurements were performed simultaneously in an apparatus that could measure three samples at a time. The specimens were mounted between two platinum blocks, which had type-S thermocouples (Pt versus Pt–10% Rh) as electrical contacts; the Pt wire heater was wound on the lower end of the holder to generate a temperature gradient along the vertical direction. Three sets of specimens and holders were contained in Al_2O_3 tubes within a $MoSi_2$ furnace, where the temperature was controlled by a Eurotherm temperature controller. The oxygen activity over the samples was controlled by using flowing gas mixtures composed of either O_2–N_2 or CO_2-forming gas (10% H_2–90% N_2). A Y_2O_3-stabilized ZrO_2 oxygen sensor was used to monitor the oxygen partial pressure of the gas mixture. Electrical conductivity measurements were made using the two-probe, four-wire Kelvin technique in which two leads carry the test signal (1 mA) and the other two measure the voltage drop. The Seebeck coefficients were determined by measuring temperature gradients and thermal emf's through the common leads of the thermocouples. The measurements were made using a data logger (Hewlett Packard 3497A data acquisition/control unit), which employs a HP-85 computer both as a control and readout device.[4]

3 Results and Discussion

3.1 Temperature dependence

DC electrical conductivity of $La(Cr,Co)O_3$ was measured in air as a function of temperature, with results shown in Fig. 1. The electrical conductivity increased with increasing temperature and Co content. The electrical conductivity of the end members of the $La(Cr,Co)O_3$ series exhibits the activated behavior expected from small-polaron transport over a wide temperature range. Previous investigations[5–7] have indicated that $LaCrO_3$ and $LaCoO_3$ perovskites conduct by the diffusion of p-type small polarons among Cr and Co ions. A small polaron is associated with a particular Cr or Co site if the ion is in the +4 valence state, rather than the stoichiometric +3 valence state.

Transport of the carrier to an adjacent unoccupied site requires transport of the lattice distortion as well. The activation energy is associated with small-polaron transport, and charge migration through the crystal occurs by an activated hopping mechanism. Two different types of small

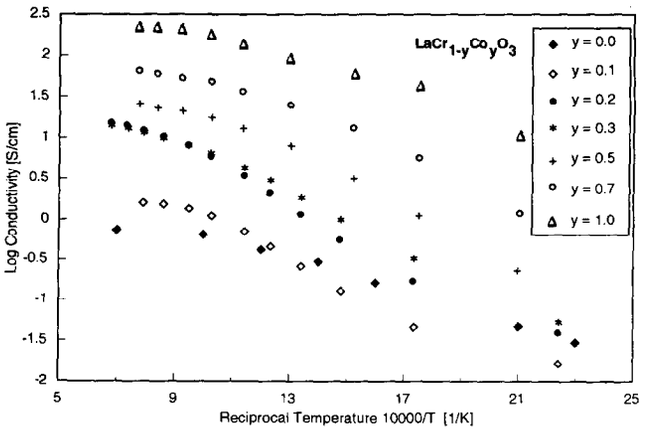

Fig. 1. DC electrical conductivity versus 10 000/T in air for $La(Cr,Co)O_3$.

polaron have been determined. The carrier is always able to jump to an adjacent unoccupied site whenever an atomic displacement favoring the jump occurs, which is called the adiabatic case, while in the non-adiabatic case the carrier can only occasionally take advantage of a favorable atomic configuration and change sites.

The mobility of charge carriers, μ, of adiabatic small polarons is given as[8]

$$\mu = [(1-C)\, e\, a^2 \nu / kT] \exp(-E_A/k/T) \qquad (1)$$

where C is the fraction of available sites occupied by charge carriers, e is the unit charge, a is the lattice spacing, ν is the vibrational frequency, k is the Boltzmann constant, T is absolute temperature, and E_A is the activation energy for hopping. The electrical conductivity, σ, is expressed as

$$\sigma = (NC)\, e\, \mu \qquad (2)$$

where N is the density of available sites. The expression for the temperature-dependent electrical conductivity of an adiabatic small-polaron material becomes

$$\sigma = [NC\,(1-C)\, e^2\, \nu\, a^2/kT] \exp(-E_A/kT) \qquad (3)$$

For materials that obey non-adiabatic small-polaron conduction, the mobility expression is given by

$$\mu = [(1-C)\, e^2\, a^2/kT]\, (4\, \pi^2 j^2/h^2)\, (\pi/4\, kTE_A)^{1/2} \exp(-E_A/kT) \qquad (4)$$

where j is the electron transfer energy and h is Planck's constant. The electrical conductivity of a non-adiabatic small-polaron material becomes

$$\sigma = [NC(1-C)\, e^2\, a^2/kT]\, (4\, \pi^2 j^2/h^2)\, (\pi/4\, kTE_A)^{1/2} \exp(-E_A/kT) \qquad (5)$$

If all of the variables in the pre-exponential term of eqns (3) and (5) are independent of temperature (or slightly temperature-dependent), a plot of log (σT) (for the adiabatic case) or log ($\sigma T^{3/2}$) (for the non-adiabatic case) versus reciprocal temperature should give a straight line, with a gradient proportional to the activation energy associated with small-polaron hops.

Plots of log (σT) versus 10 000/T and log ($\sigma T^{3/2}$) versus 10 000/T for La(Cr,Co)O_3 compositions covering the entire temperature range studied are shown in Figs 2 and 3, respectively. The two plots are very similar, showing substantial linearity for the compositions. Linear regression was applied to calculate the activation energies and evaluate the linearity of plots for the compositions. Calculated values for the activation energies are given for each case in Table 1. The conductivity of the compositions of the La(Cr,Co)O_3 series does exhibit the activated behavior expected from small-polaron transport over a wide temperature range, with $\sigma T^{3/2}$ giving a slightly better fit than σT. Linear regression was used to evaluate the linearity of the plots. The linearity was slightly higher for the non-adiabatic case (Fig. 3) than for the adiabatic case (Fig. 2). R^2 values are included in Table 1 for

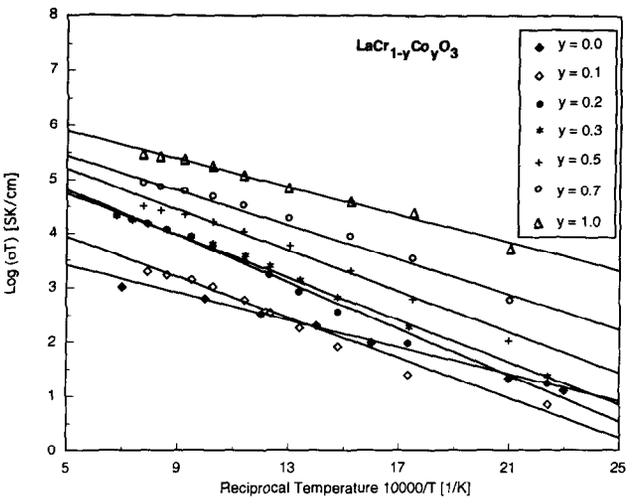

Fig. 2. Log σT versus 10 000/T for La(Cr,Co)O_3.

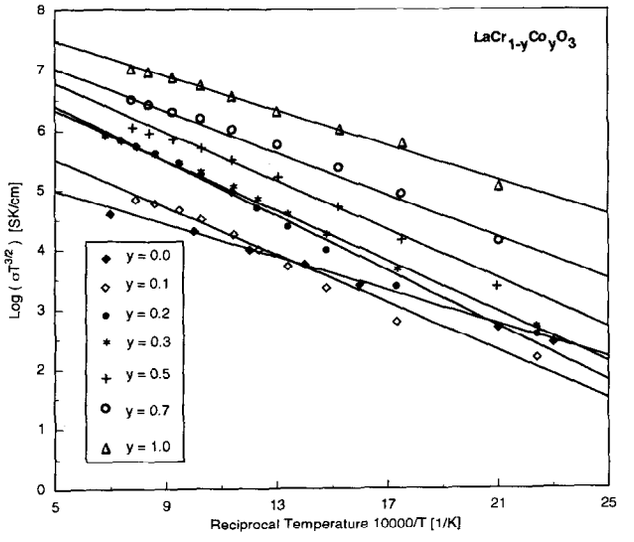

Fig. 3. Log $\sigma T^{3/2}$ versus 10 000/T for La(Cr,Co)O_3.

Table 1. Activation energies for La(Cr,Co)O_3

	Activation energy (eV)			
Composition $LaCr_{1-y}Co_yO_3$	*Adiabatic case*	*Non-adiabatic case*	*Adiabatic case*	*Non-adiabatic case*
$y = 0.0$	0·25	0·28	0·9930	0·9966
$y = 0.1$	0·37	0·40	0·9786	0·9805
$y = 0.2$	0·42	0·46	0·9894	0·9900
$y = 0.3$	0·39	0·42	0·9958	0·9972
$y = 0.5$	0·37	0·41	0·9869	0·9912
$y = 0.7$	0·32	0·35	0·9843	0·9903
$y = 1.0$	0·26	0·29	0·9875	0·9915

both cases. The greater the magnitude of R^2, the better the fit of the data to the linear function. Evaluation of the linearity of plots for compositions in La(Cr,Co)O_3 indicated that the electrical conduction occurs via the non-adiabatic small-polaron mechanism.

Although the activation energies of the end members are similar, $LaCoO_3$ has a high-temperature conductivity value much higher than that of $LaCrO_3$. Despite the larger intrinsic electronic conductivity of $LaCoO_3$, a small substitution of Co for Cr in $LaCrO_3$ resulted in a sharp drop in low-temperature conductivity from that exhibited by either end member (see Fig. 1). This minimum occurs at a Co concentration of 10 mol%. This small substitution of Co also resulted in a strong temperature dependence with increased gradient. The maximum gradient observed occurs in the 20 mol% Co composition and corresponds to an activation energy of 0·46 eV. As can be seen from Table 1, the activation energy increases with Co content to a maximum at 20 mol% and then linearly decreases as Co content increases. The substitution of small amounts of Co for Cr has been found to cause the low-temperature electrical conductivity to drop orders of magnitude below that of either end member and increase in activation energy. This is probably due to the difference in the electronic structure of Co and Cr ions. The Co sites also have lower small-polaron site energies as compared to Cr sites. In the case of a low concentration of Co, the lower-energy Co sites act as traps for carriers diffusing among Cr sites at low temperature. Therefore, the activation energy for conduction is increased from that of $LaCrO_3$. At higher Co concentrations, direct transport among Co sites becomes possible and conductivity increases and activation energy decreases. The electrical conductivity of all compositions increased to an asymptotic value dependent upon the amount of Co present as the temperature was increased. A possible explanation for this involves considering the different spin states of Co. The low spin (s = 0) state is the most stable and predominates at temperatures below 900°C. As the temperature increases, higher spin states of Co^{3+} (s = 1, s = 2) become populated. This transition probably leads to hopping between Co-sites and neighboring Cr-sites. Therefore, the electrical conductivity at higher temperatures increased with Co concentration.

The DC electrical conductivity of $La_{1-x}Ca_xCR_{0.9}Co_{0.1}O_3$ and $La_{1-x}Ca_xCr_{0.8}Co_{0.2}O_3$ (with x = 0·1 and 0·2) was measured in air as a function of temperature, with the results shown in Figs 4 and 5, respectively, as log(σ) as a function of reciprocal temperature. Plots of log (σT) versus 10 000/T and log ($\sigma T^{3/2}$) versus 10 000/T for

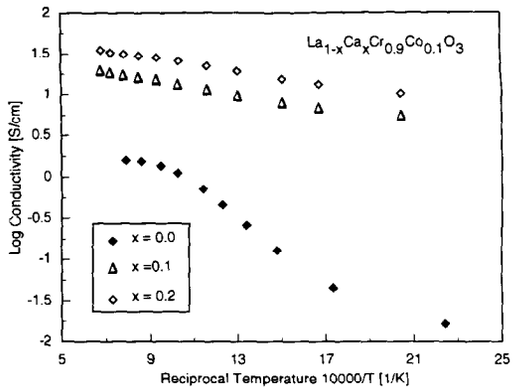

Fig. 4. DC electrical conductivity of $La_{1-x}Ca_xCr_{0.9}Co_{0.1}O_3$ as a function of Ca content and temperature.

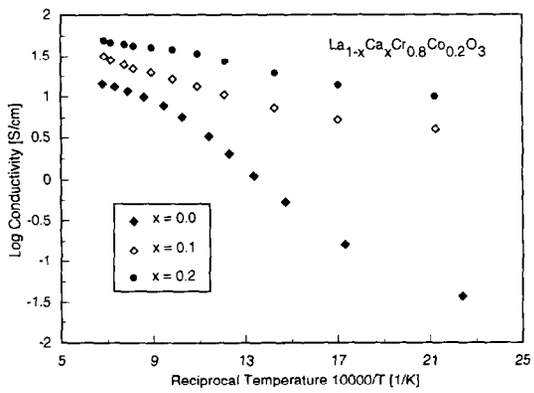

Fig. 5. DC electrical conductivity of $La_{1-x}Ca_xCr_{0.8}Co_{0.2}O_3$ as a function of Ca content and temperature.

$La_{1-x}Ca_xCr_{0.9}Co_{0.1}O_3$ are shown in Figs 6 and 7, respectively. The two plots are very similar, showing slightly higher linearity for the adiabatic case. Thus, for the system $La_{1-x}Ca_xCr_{0.9}Co_{0.1}O_3$, the high linearity of the plots is consistent with the assumption that electrical conduction in these compositions occurs via the adiabatic small-polaron mechanism (see Table 2). Log (σT) versus 10 000/T and log ($\sigma T^{3/2}$) versus 10 000/T for $La_{1-x}Ca_xCr_{0.8}Co_{0.2}O_3$ are also plotted in Figs 8 and 9, respectively. The linearity of the plots are again consistent with the assumption that electrical

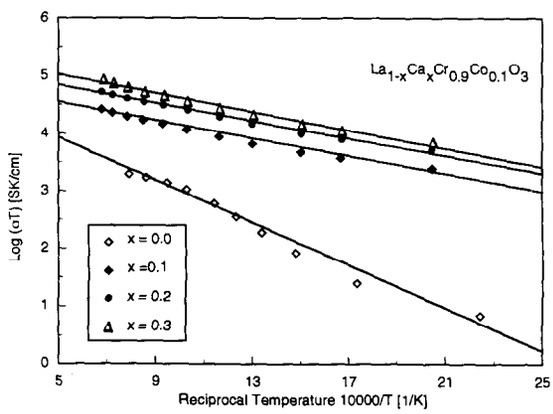

Fig. 6. Log σT versus 10 000/T for $La_{1-x}Ca_xCr_{0.9}Co_{0.1}O_3$.

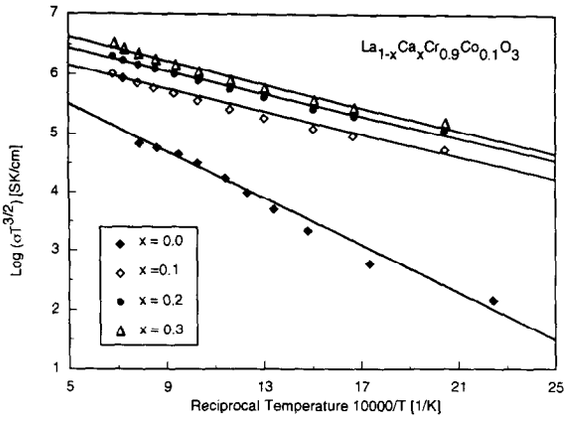

Fig. 7. Log $\sigma T^{3/2}$ versus 10000/T for $La_{1-x}Ca_xCr_{0.9}Co_{0.1}O_3$.

conduction occurs via the adiabatic small-polaron mechanism. There was only one composition (x = 0·1) which had the greater magnitude of R^2 in the non-adiabatic case. This might be due to the experimental error, since the rest of the compositions yielded a better fit of the data to the linear function with the adiabatic small-polaron mechanism.

Activation energies for hopping for adiabatic and non-adiabatic cases were calculated from Figs 6–9 and tabulated in Table 2. The activation energies were slightly higher for the non-adiabatic case than for the adiabatic case. As can be seen, with a

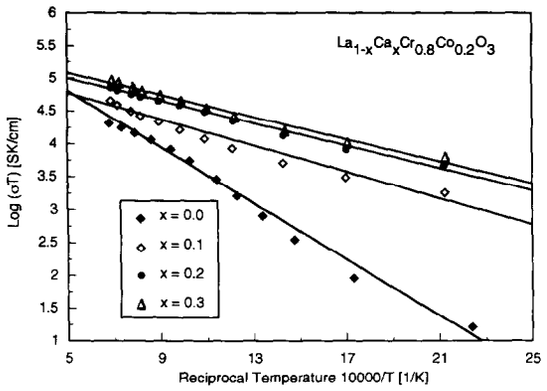

Fig. 8. Log σT versus 10000/T for $La_{1-x}Ca_xCr_{0.8}Co_{0.2}O_3$.

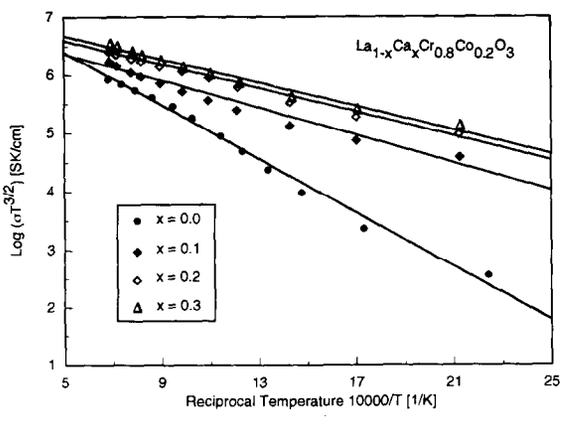

Fig. 9. Log $\sigma T^{3/2}$ versus 10000/T for $La_{1-x}Ca_xCr_{0.8}Co_{0.2}O_3$.

Table 2. Activation energies for (La,Ca)(Cr,Co)O_3

Composition $La_{1-x}Ca_xCr_{1-y}Co_yO_3$	*Activation energy (eV)*			
	Adiabatic case	*Non-adiabatic case*	*Adiabatic case*	*Non-adiabatic case*
x = 0·1; y = 0·1	0·16	0·19	0·9825	0·9818
x = 0·2; y = 0·1	0·15	0·19	0·9912	0·9895
x = 0·3; y = 0·1	0·16	0·19	0·9850	0·9836
x = 0·1; y = 0·2	0·20	0·23	0·9678	0·9688
x = 0·2; y = 0·2	0·17	0·20	0·9915	0·9905
x = 0·3; y = 0·2	0·17	0·20	0·9817	0·9811

Ca content of 10–30 mol%, all Co-content levels have essentially the same activation energy. The additional substitution of Ca for La in the La(Cr,Co)O_3 eliminated the increase in activation energy that was observed with Co substitution for Cr. The substitution of 10 mol% Ca for La in the La(Cr,Co)O_3 series increased the conductivity by approximately 10%, which was anticipated in view of a carrier density increase of 10% in accordance with Verway's principle. As in the case of $La_{1-x}Ca_xCrO_3$ and $La_{1-x}Ca_xCO_3$, the substitution of Ca for La in La(Cr, Co)O_3 should result in the formation of Cr^{4+} and Co^{4+} in order to preserve the electrical neutrality. Formation of both Cr^{4+} and Co^{4+} increases the small-polaron concentration and decreases the activation energy for conduction.

Thermopower measurements were made to determine the type and concentration of charge carriers. Figures 10–12 show the Seebeck coefficient plotted as a function of temperature for La(Cr,Co)O_3, $La_{1-x}Ca_xCr_{0.9}Co_{0.1}O_3$, and $La_{1-x}Ca_xCr_{0.8}Co_{0.2}O_3$, respectively. In La(Cr,Co)O_3, the substitution of Co for Cr significantly decreased the Seebeck coefficient, indicating that Co substitution for Cr increases the carrier concentration. As the Co content increased, the Seebeck

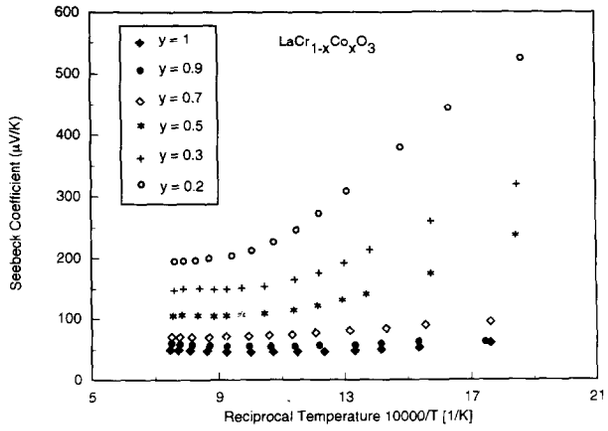

Fig. 10. Seebeck coefficients of La(Cr,Co)O_3 as a function of Co and temperature.

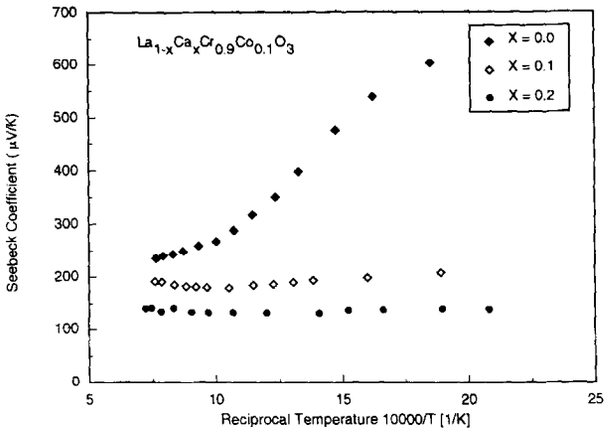

Fig. 11. Seebeck coefficients of $La_{1-x}Ca_xCr_{0.9}Co_{0.1}O_3$ as a function of Ca and temperature.

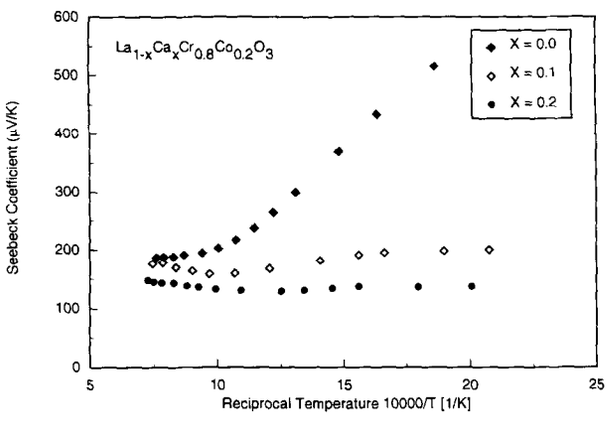

Fig. 12. Seebeck coefficients of $La_{1-x}Ca_xCr_{0.8}Co_{0.2}O_3$ as a function of Ca and temperature.

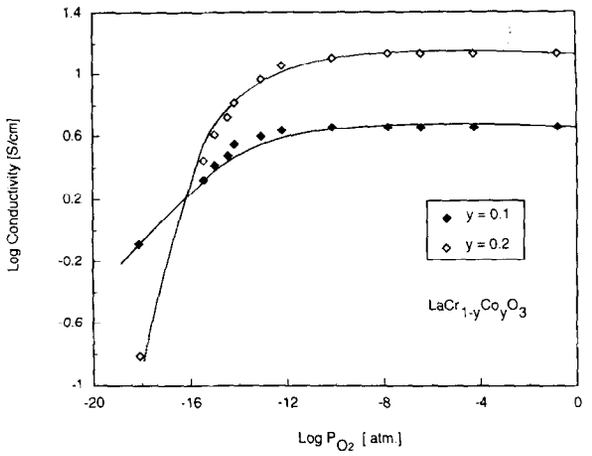

Fig. 13. Log σ versus log oxygen activity for La(Cr,Co)O_3 at 1000°C.

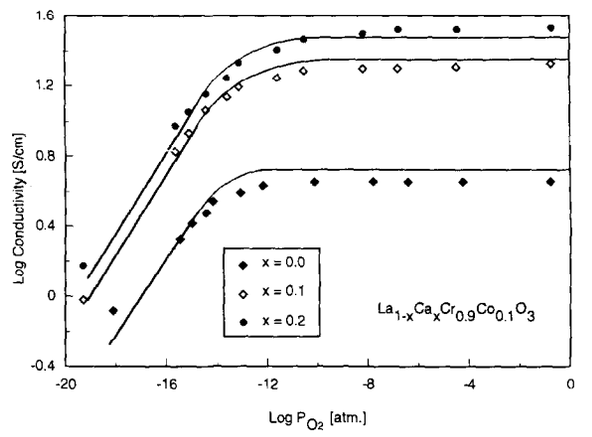

Fig. 14. Log σ versus log oxygen activity for (La,Ca)(Cr,Co)O_3 at 1000°C.

coefficient showed temperature-independent behavior, indicating that the carrier mobility, rather than the carrier concentration, was thermally activated. According to Heikes' formula, this type of behavior indicates a small-polaron conduction mechanism which agrees with electrical conductivity measurements. In the cases of $La_{1-x}Ca_xCr_{0.9}Co_{0.1}O_3$ and $La_{1-x}Ca_xCr_{0.8}Co_{0.2}O_3$, introduction of Ca significantly decreased the Seebeck coefficient, which became temperature-independent.

3.2 Oxygen-activity dependence

DC electrical conductivity measurements for $La_{1-x}Ca_xCr_{1-y}Co_yO_3$ (x = 0·0, 0·1, 0·2, 0·3 and y = 0·1, 0·2) were made as a function of oxygen activity at 1000°C. The results are shown in Figs 13 and 14. The electrical conductivity data showed similar oxidation–reduction behavior. In the high oxygen-activity region, within the experimental error the electrical conductivity was nearly constant. The electrical conductivity decreased as a function of oxygen activity to the one-quarter power as reduction progressed. The constant electrical conductivity that exists in the high oxygen-activity region may be easily understood if it is assumed that the carrier concentration and electronic compensation predominates. In the low oxygen-activity region, oxygen vacancies are formed and the electrical conductivity begins to decrease as a result of ionic compensation.

The defect chemistry of oxides shows how the defect structure and electrical conductivity change as they equilibrate under various oxygen activities at elevated temperatures. The following model is adopted from the model developed for Mg-doped $LaCrO_3$[5] in order to explain the electrical conductivity of $La_{1-x}Ca_xCr_{1-y}Co_yO_3$ (where y is less than 0·3) as a function of oxygen activity. In the $La_{1-x}Ca_xCr_{1-y}Co_yO_3$, the Co^{3+} substitutes for Cr^{3+}, and Ca^{2+} substitutes for La^{3+}. The acceptor Ca^{2+} substitutes for La^{3+}. The acceptor Ca^{2+} possesses one effective negative charge which can be compensated for either by Cr^{3+}–Cr^{4+} or Co^{3+}–Co^{4+} transitions, or by the formation of oxygen vacancies. If such a substitution is compensated for by the formation of oxygen vacancies, no contribution to the electronic conductivity is anticipated.

Since cations and anions are of comparable size, it can be assumed that Schottky is native defect, and the Schottky reaction (using the Kroger–Vink notations[9]) for this composition is expressed by

$$\text{nill} = V'''_{La} + V'''_{Cr,Co} + 3\ V^{\cdot\cdot}_{O} \quad (6)$$

$$K_s = [V'''_{La}][V'''_{Cr,Co}][V^{\cdot\cdot}_{O}]^3 \quad (7)$$

Since this is a closed system, the cation stoichiometry must remain constant, therefore, $[V_{La}] = [V_{Cr,Co}] = [V_M]$ throughout the entire region.

$$K_s = [V'''_M]^2\,[V^{\cdot\cdot}_O]^3 \quad (8)$$

The p-type non-stoichiometric reaction is given by

$$3/2\ O_2 = V'''_{La} + V'''_M + 6\,\dot{h} + 3\ O_o \quad (9)$$

$$K_9 = [V'''_{La}]\,[V'''_M]\,p^6\,P_{O_2}^{-3/2} \quad (10)$$

When Ca^{2+} is substituted for La^{3+}, the Ca^{2+} will possess one effective negative charge which can be compensated for either by a B^{3+}–B^{4+} transition or by the formation of oxygen vacancies. This leads to the following electrical neutrality condition:

$$2\,[V^{\cdot\cdot}_O] + p = 6\,[V'''_M] + [Ca'_M] \quad (11)$$

At high oxygen activity, assuming that both $[V_O]$ and $[V_M]$ are smaller than the acceptor content, the neutrality condition becomes

$$p = [Ca'_M] \quad (12)$$

and from eqns 8, 10 and 12

$$[V'''_M] = K_9^{1/2}\,P_{O_2}^{3/4}/[Ca'_M]^3 \quad (13)$$

$$[V^{\cdot\cdot}_O] = K_S^{1/3}\,[Ca'_M]^2\,P_{O_2}^{-1/2}/K_9^{1/3} \quad (14)$$

respectively.

At low oxygen activities, oxygen may be lost and ionic compensation takes place through the formation of oxygen vacancies. In this case the electrical neutrality condition becomes

$$p = [Ca'_M] - 2[V^{\cdot\cdot}_O] \quad (15)$$

This condition can be expressed by

$$La_{1-y}Ca'_yM^x_{1-y}M^{\cdot}_yO_3 = La_{1-y}Ca'_yM^x_{1-y+2x}M^{\cdot}_{y-2x}V^{\cdot\cdot}_{Ox}O_{3-x} + \tfrac{1}{2}\,xO_2$$

or

$$O_O + 2\ M^{\cdot}_M = 2\ M_M + V^{\cdot\cdot}_O + 1/2\ O_2 \quad (16)$$

where y is the amount of acceptor and x is the concentration of oxygen vacancies. The equilibrium constant for reaction (16) can be expressed as

$$K_{16} = [M_M]^2\,[V^{\cdot\cdot}_O]\,P_{O_2}^{1/2}/[M^{\cdot}_M]^2 \quad (17)$$

which in terms of mole fractions becomes

$$K_{16} = (1-y+2x)^2\,x\,P_{O_2}^{1/2}/(y-2x)^2 \quad (18)$$

Equation (18) can be solved to yield

$$2x = y - \{P_{O_2}^{1/2}\,[(8y\,K_{16}\,P_{O_2}^{-1/2} + 1)^{1/2} - 1]/4\,K_{16}\} \quad (19)$$

The electrical conductivity for p-type materials is given by

$$\sigma = e\,p\,\mu \quad (20)$$

where e is the electron charge, μ is the mobility, and p is the concentration of carriers which, from the model, is equal to $(y–2x)$. Thus eqn (19) can be rearranged to give

$$\sigma = e\mu P_{O_2}^{1/2}\{[(8\,yK_{16}\,P_{O_2}^{-1/2} + 1)^{1/2} - 1]/4\}K_{16} \quad (21)$$

At the high oxygen-activity region, eqn (19) reduces to $x = 0$ and eqn (21) reduces to $\sigma = e\,y\,\mu$, whereas in the low oxygen-activity region the respective equations are reduced to

$$p = (y\text{-}2x)/y = P_{O_2}^{1/4}/(2y\,K_{16})^{1/2} \quad (22)$$

or

$$\sigma = (e\,\mu\,y^{1/2}\,P_{O_2}^{1/4})/2K_{16} \quad (23)$$

and

$$\sigma/\sigma_R = P_{O_2}^{1/4}/(2y\,K_{16})^{1/2} \quad (24)$$

where σ_R is the electrical conductivity at 1 atm oxygen.

The equilibrium constant K_{16} can be found by combining the electrical conductivity experimental data and eqn (24). The theoretical curves can be generated by using eqn (24) and the calculated values of K_{16}. The individual symbols in Figs 13–14 represent the experimental data, while the lines are the calculated curves. The equilibrium constants used to generate these lines are listed in Table 3. It is clear that the electrical conductivity decreases with decreasing oxygen activity as $P_{O_2}^{1/4}$, as the electrical compensation changes from electronic to ionic. All of the compositions showed the same behavior. The oxygen-activity dependence on conductivity was small at high oxygen activities; as oxygen activity decreased, a break in electrical conductivity at 10^{-10} atm and 1000°C was observed, then the electrical conductivity decreased as $P_{O_2}^{1/4}$. Compositions $La_{1-x}Ca_xCr_{1-y}Co_yO_3$ with x = 0·0–0·3 and y = 0·0–0·2 are stable towards dissociation

Table 3. Equilibrium constants calculated from defect model at 1000°C

Composition	*Log equilibrium constant*
$LaCr_{0.9}Co_{0.1}O_3$	–4·8
$La_{0.9}Ca_{0.1}Cr_{0.9}Co_{0.1}O_3$	–5·8
$La_{0.8}Ca_{0.2}Cr_{0.9}Co_{0.1}O_3$	–6·1
$LaCr_{0.8}Co_{0.2}O_3$	–4·1
$La_{0.9}Ca_{0.1}Cr_{0.8}Co_{0.2}O_3$	–4·8
$La_{0.8}Ca_{0.2}Cr_{0.8}Co_{0.2}O_3$	–5·2

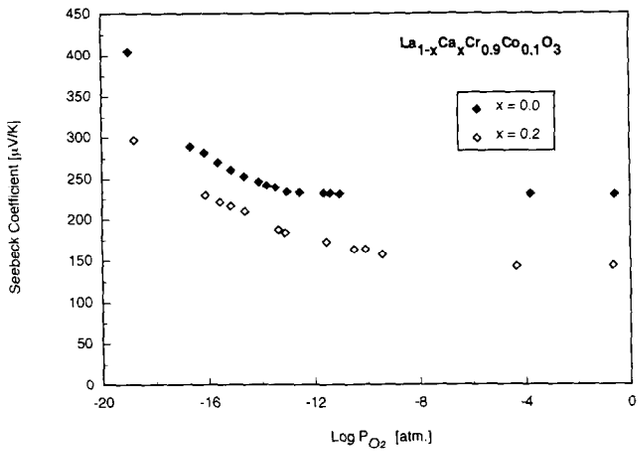

Fig. 15. Seebeck coefficient as a function of oxygen activity for $LaCr_{0.9}Co_{0.1}O_3$ at 1000°C.

in forming gas at 1000°C, even though the electrical conductivity decreases.

Seebeck measurements were also made as a function of oxygen activity at 1000°C. The results for compositions $(La,Ca)(Cr,Co)O_3$ are shown in Fig. 15 . The Seebeck coefficients in all cases were positive, indicating p-type conductivity. Increasing the Co substitution for Cr decreased the Seebeck coefficients. In accordance with the electrical conductivity, the Seebeck coefficient remains constant until the low P_{O_2} region is reached. At this point, the Seebeck coefficient rapidly increases at the transition knee because of its inverse relationship with the carrier concentration. The location of the transition knee shifted to a higher P_{O_2} with increasing Co and Ca concentration in both the Seebeck and electrical conductivity data. For the high P_{O_2} region, the carrier concentration is controlled by the acceptor content p = [Ca'] and electronic compensation predominates. Any temperature dependence of the electrical conductivity is therefore determined by mobility. It should be noted that in eqn (24), the mobility was assumed to be independent of oxygen activity. This is an important feature of the model if the calculated equilibrium constants are to be regarded as correct.

4 Conclusions

The electrical conductivity as measured in air from 100 to 1100°C increased with increasing Co and Ca content. At 1000°C, values from 1·5 S/cm (for $LaCr_{0.9}Co_{0.1}O_3$) to 50 S/cm (for $La_{0.7}Ca_{0.3}Cr_{0.9}Co_{0.1}O_3$) were measured. The Seebeck coefficients were positive, indicating p-type conductivity. The substitution of Co for Cr significantly decreased the Seebeck coefficients, indicating that Co substitution for Cr increased the carrier concentration. Additional Ca substitution for La resulted in a further decrease in the Seebeck coefficient. Seebeck coefficients then exhibited a temperature-independent behavior, indicating that the carrier mobility, rather than carrier concentration, was thermally activated. The results indicated that the electrical conduction in $La(Cr,Co)O_3$ and $(La,Ca)(Cr,Co)O_3$ occurs via the non-adiabatic and adiabatic small-polaron mechanisms, respectively.

At 1000°C the oxygen activity dependence upon conductivity was small at high oxygen activities; as oxygen activity decreased, a break at 10^{-10} atm was observed, at which point the electrical conductivity began decreasing as $P_{O2}^{1/4}$, following the model previously proposed for $LaCrO_3$.

References

1. Koc, R. & Anderson, H. U., Liquid phase sintering of $LaCrO_3$. *J. Eur. Ceram. Soc.*, **9** (1992) 285–92.
2. Koc, R. & Anderson, H. U., Electrical conductivity and Seebeck coefficient of $(La,Ca)(Cr,Co)O_3$. *J. Mater. Sci.*, **27** (1992) 5477–82.
3. Pechini, M., Method of preparing lead and alkaline earth titanates and niobates and coatings using the same to form a capacitor. US Patent 3 330 697, 1967.
4. Carini, G., An apparatus for the measurement of DC electrical and seebeck coefficient of semiconductors as a function of high temperature and oxygen activity. MS Thesis, University of Missouri-Rolla (1988).
5. Flandermeyer, B. K., Thermogravimetric and electrical conductivity studies of Mg-doped $LaCrO_3$ and La-doped $SrTiO_3$. PhD Thesis, University of Missouri-Rolla (1984).
6. Karim, D. P. & Aldred, A. T., Localized level hopping transport in $La(Sr)CrO_3$. *Phys. Rev. B*, **20**(6) (1979) 2255–63.
7. Taguchi, H., Shimada, M. & Koizumi M., Electrical properties in the system $(La_{1-x}Ca_x)CoO_3$ $(0{\cdot}1<x<0{\cdot}5)$. *J. Solid State Chem.*, **44** (1982) 254–6.
8. Stevenson, W. J., Electrical and structural properties of compositions in the systems $Y_{1-x}Ca_xMnO_3$ and $La_{1-x}Ca_xMnO_3$. PhD Thesis, University of Missouri-Rolla (1991).
9. Kroger, F. A. & Vink, H. J., *Solid State Physics*, Vol. 3, eds F. Seitz & D. Turnbull. Academic Press, New York, 1965, p. 307.